FULL PAPER *Pathology*

Histological and immunohistochemical evaluation of stroma variations and their correlation with the Ki-67 index and expressions of glucose transporter 1 and monocarboxylate transporter 1 in canine thyroid C-cell carcinomas

Yoshio KAWAMURA[1)], Hiroko MIZOOKU[1)], Minoru OKAMOTO[2)], Kazuya MATSUDA[1)], Tetsuo OMACHI[4)], Kazuko HIRAYAMA[1)], Tsuyoshi KADOSAWA[3)] and Hiroyuki TANIYAMA[1)]*

[1)]*Department of Veterinary Pathology, Rakuno Gakuen University, 582 Midori-machi, Bunkyo-dai, Ebetsu, Hokkaido 069–8501, Japan*
[2)]*Department of Veterinary Immunology, Rakuno Gakuen University, 582 Midori-machi, Bunkyo-dai, Ebetsu, Hokkaido 069–8501, Japan*
[3)]*Department of Veterinary Clinical Oncology, Rakuno Gakuen University, 582 Midori-machi, Bunkyo-dai, Ebetsu, Hokkaido 069–8501, Japan*
[4)]*Patho LABO Co., Ltd., 9–400, Omurokogen, Ito, Shizuoka 413–0235, Japan*

(Received 30 October 2015/Accepted 4 December 2015/Published online in J-STAGE 3 January 2016)

ABSTRACT. Canine thyroid C-cell carcinomas (CTCCs) are malignant tumors derived from calcitonin-producing C-cells of the thyroid gland. This study aimed to investigate the histological diversity of CTCCs from the viewpoint of stroma variations and to investigate their components by histological and immunohistochemical analyses including semiquantitative analysis of the density of microvessels (MVs) and α-SMA-positive cell count. Moreover, we examined whether the variations correlated with the Ki-67 index and expressions of glucose transporter 1 (GLUT-1) and monocarboxylate transporter 1 (MCT-1). Three stroma types (reticular, R, nest, N, and trabecular, T) were observed in CTCCs, and 21 cases were divided into 3 variations based on their combinations: mixed R and N (R/N) (n=7), simple N (n=7) and mixed T and N (T/N) (n=7). Immunohistochemically, stroma types depended on morphological features of α-SMA/fibronectin/laminin/collagen type IV-positive stroma cells. The density of MVs in R/N tended to be highest, and the density of those in N was significantly higher than the density of those in T/N (P=0.028). The α-SMA-positive cell count for N tended to be the lowest among the 3 variations. The Ki-67 index for R/N was significantly higher than those of the other variations (vs. N, P=0.007; vs. T/N, P=0.03), and that for T/N tended to be higher than that for N. Although there were no significant differences, GLUT-1 and MCT-1 expressions tended to be low in N. We concluded that stroma variations reflect tumor cell proliferation and expressions of GLUT-1 and MCT-1 in CTCCs.
KEY WORDS: canine, C-cell carcinoma, endocrine, thyroid cancer

doi: 10.1292/jvms.15-0619; *J. Vet. Med. Sci.* 78(4): 607–612, 2016

Canine thyroid C-cell carcinomas (CTCCs) are malignant tumors derived from calcitonin-producing C-cells of the thyroid gland [2, 7, 8, 12, 13]. A previous study showed that some histological and cytological variants observed in CTCCs varied in different areas of the same neoplasm; however, there was no mention of any relationship with tumor cell activity [13]. Generally, tumor cell activity is presumed from the differentiation degree or pleomorphic shapes of tumor cells themselves; however, this is difficult in thyroid C-cells because of their simple cytological features. To solve this problem, a new viewpoint is needed. In recent years, the mutual relationships between tumor parenchyma cells and the stroma have been revealed [10, 11, 16]; therefore, we focused on whether the difference in histological stroma types affects tumor cell activity in CTCCs.

Tumor cell proliferation and angiogenesis are important factors for tumor cell survival. They are regulated by tumor microenvironments that include not only their own components, such as fibroblasts or extracellular matrixes (ECMs), but also various factors, such as oxygenic conditions and nutrient supply [10, 16, 17]. Therefore, the present study focused on the relations of stroma type, stromal components and angiogenesis with tumor cell activity, including both tumor cell proliferation and metabolism.

Tumor cell metabolism reflects both tumor cell activity and microenvironments. Glucose transporter 1 (GLUT-1) is a major isoform of GLUTs that uptakes glucose into cytoplasm by expressing on the cell surface [1, 14]. Monocarboxylate transporter 1 (MCT-1) is known as a transmembrane transporter that facilitates L-lactic acid entry into or efflux out of cells depending on their metabolic state [6, 15]. These proteins are important to tumor cell survival and are overexpressed in many canine tumors including malignant melanomas, mammary gland carcinomas and histiocytic sarcomas [1, 5, 15]; however, they have not been investigated in CTCCs.

The aim of this study was to reveal the detailed stroma types and their components in CTCCs, and to evaluate how the combinations of stroma types (stroma variations) are correlated with tumor cell proliferation and expressions of GLUT-1 and MCT-1 by immunohistochemical analysis.

*CORRESPONDENCE TO: TANIYAMA, H., Department of Veterinary Pathology, Rakuno Gakuen University, 582, Bunkyodai-Midori-machi, Ebetsu, Hokkaido 069–8501, Japan.
e-mail: taniyama@rakuno.ac.jp

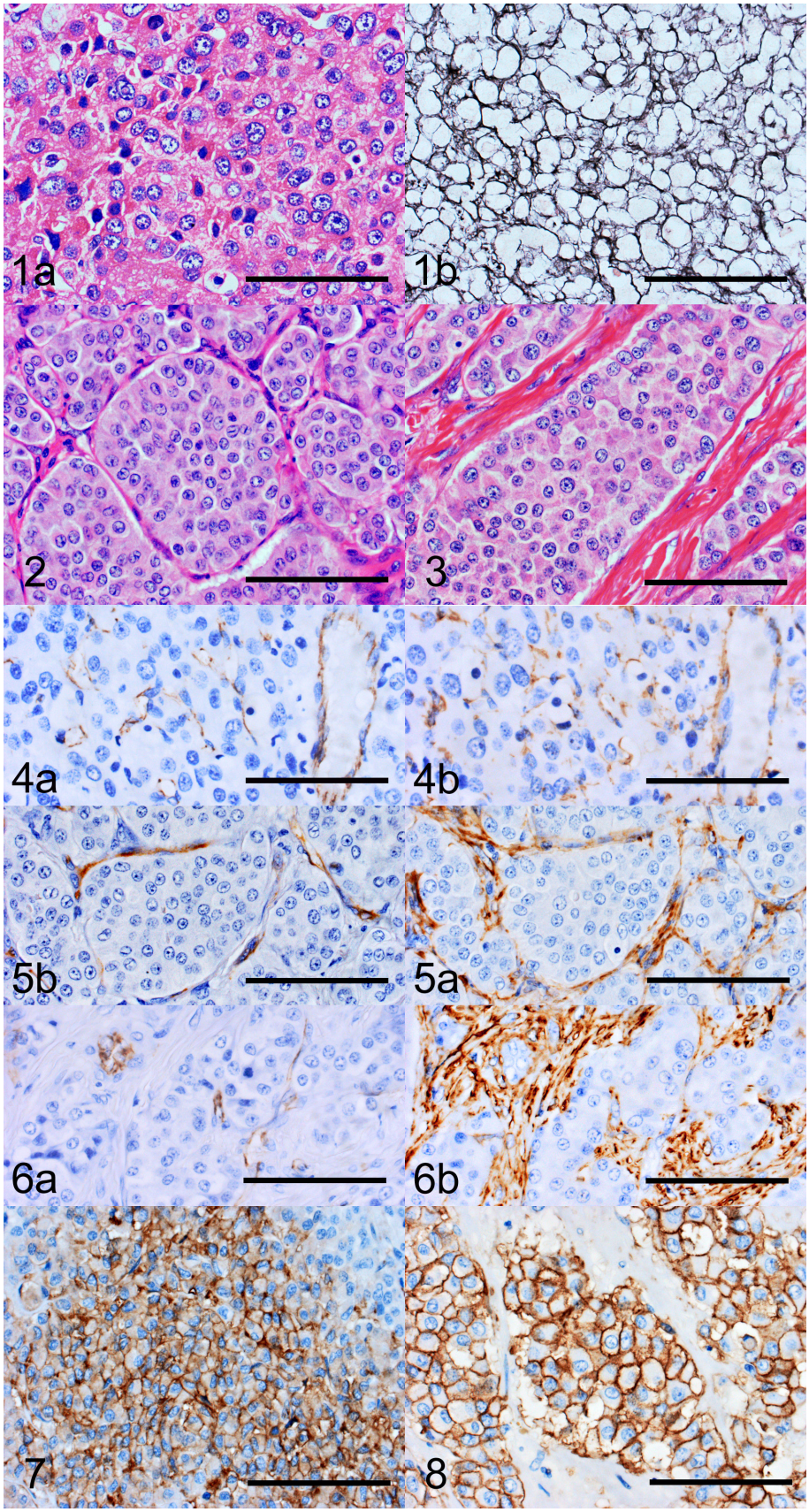
1a
1b
2
3
4a
4b
5b
5a
6a
6b
7
8

MATERIALS AND METHODS

Animals and histology: After surgical exclusion based on clinical diagnosis as thyroid carcinomas, all 21 cases were diagnosed as CTCCs based on histopathological features and immunohistochemical examination using anti-human calcitonin antibodies. Sections (4 μm) were stained with hematoxylin and eosin (HE) and periodic acid-methenamine-silver (PAMS) stain for visualization of collagen and reticular fibers. By histological examination at ×200 magnification, stroma types of CTCCs were divided into 3 types: reticular (R), nest (N) and trabecular (T). The R type had thin reticular fibers visualized with PAMS stain circumscribing single or small groups (no more than 2 to 3 cells) of tumor cells (Fig. 1a and 1b). The N type had a nest-form collagenous stroma of various thicknesses surrounding several to dozens of tumor cell groups (Fig. 2). The T type had a thick trabecular-form straight to disarrayed collagenous stroma dividing several to dozens of tumor cells (Fig. 3).

Immunohistochemistry (IHC): Immunohistochemical staining was examined by the avidin-biotin peroxidase complex (ABC) procedure. Sections (4 μm) were dewaxed in xylene and hydrated through graded alcohols. To remove endogenous peroxidase, sections were immersed in 3% hydrogen peroxide solution at room temperature for 10 min. The sections were incubated in primary antibody solution. Details of the primary antibodies used are shown in Table 1. After washing with PBS, sections were incubated in secondary antibody solution at room temperature for 30 min. Following incubation, sections were reacted with VECTASTAIN Elite ABC Kit (Vector Laboratories, Burlingame, CA, U.S.A.) at room temperature for 30 min. Visualization was accomplished using 0.05% 3,3-diaminobenzidine solution. Mayer's hematoxylin stain was used as a counterstain. Sections without the primary antibody were subjected to the same procedures for the negative control.

Semiquantitative analysis of immunohistochemistry: In this study, the term "microvessels" (MVs) was used to describe fine vessels surrounded by a few pericytes. To visualize MVs clearly, the endothelial cells of MVs were detected by an immunohistochemical technique using anti-human CD31 antibody. The Ki-67 index was calculated for the percentage of Ki-67-positive tumor cells, and scoring was performed by manual counting. The semiquantitative evaluation used the "hot spots" identified in five areas at ×40 magnification in histological variants of each case. [17]. Density of MVs, α-SMA-positive cell count and Ki-67 index were scored by counting at ×200 (0.139 mm^2/field), ×400 (0.037 mm^2/field) and ×400 magnifications, and immunohistochemical staining was evaluated on the basis of a distinct immunoreaction on the cell membrane for GLUT-1 and MCT-1 without necrosis. The immunoreactive tumor cells for GLUT-1 and MCT-1 were scored for each specimen according to the following scoring system: 0=no reactive cells, 1=focal reactive cells and 2=multifocal or diffuse reactive cells.

Statistical analysis: Statistical analyses among stroma variations were performed using a nonparametric test (Kruskal-Wallis test) and multiple comparison tests (Scheffe test). The significance level was set at 5%.

RESULTS

Animal population data: This retrospective study was conducted with formalin-fixed, paraffin-embedded samples from 21 cases of thyroid C-cell carcinoma diagnosed in 21 dogs (9 males and 12 females) with unilateral thyroidectomy (13 right, 7 left; one case unknown). No dogs were treated with chemotherapy or radiotherapy before surgical treatment. The mean age was 9.1 years (range, 6–13 years), and the mean tumor maximum diameter was 5.5 cm (range, 1.6–10 cm). The mean period from first recognition of tumors by the owner to surgical treatment was 123 days (range, 1–665 days). Summaries of the animal population are shown in Supplementary Table 1.

Histological findings: By histological examination in more than 10 fields at ×100 magnification, the 21 cases were divided into the following 3 variations based on the combination of stroma types: mixed R and N (R/N; n=7), simple N (n=7) and mixed T and N (T/N; n=7) variations. Although the ratios of the mixed types were diverse for every case, they were mixed without completely separating. Aggressive extracapsular invasions were observed in 2 cases of R/N.

Fig. 1. CTCC, dog, No. 1, R-type stroma: Tumor cells arranged in sheet forms with rods- to oval-shaped nuclear cells. HE. (b) Reticular fibers circumscribing single or small groups of tumor cells. PAMS. Bar=50 μm.

Fig. 2. CTCC, dog, No. 13, N-type stroma. Collagenous stroma of various thicknesses with a few layered spindle-shaped cells and microvessels surrounding groups of tumor cells. HE. Bar=50 μm.

Fig. 3. T CTCC, dog, No. 17, T-type stroma. Thick straight to disarray collagenous fibers with spindle-shaped and linear cells; microvessels penetrating tumor cell groups. HE. Bar=50 μm.

Fig. 4. CTCC, dog, No. 1, R-type region: (a) CD31-positive endothelial cells of MVs scattered among tumor cells. IHC. (b) Scattered α-SMA-positive stromal cells having dendritic cytoplasm (serial section of a). IHC. Bar=50 μm.

Fig. 5. CTCC, dog, No. 17, N-type region: (a) CD31-positive endothelial cells of MVs surrounding the tumor cells groups entirely. IHC. (b) Alpha-SMA-positive spindle-shaped cells surrounding the entire circumference of tumor cell groups. IHC. Bar=50 μm.

Fig. 6. CTCC, dog, No. 17, T-type region. (a) CD31-positive endothelial cells of MVs poorly branched and penetrating through thick collagenous bundles. (b) Alpha -SMA-positive spindle-shaped linear cells parallel and extending long and straight along the collagenous bundles (serial section of a). IHC. Bar=50 μm.

Fig. 7. CTCC, dog, No. 6, R/N variation. Cytoplasmic membrane of tumor cells expressing GLUT-1. IHC. Bar=50 μm.

Fig. 8. CTCC, dog, No. 20, T/N variation. Cytoplasmic membrane of tumor cells expressing MCT-1. IHC. Bar=50 μm.

Table 1. Details of the primary antibodies for immunohistochemistry

Antibodies	Antibody type (clone)	Dilution	Antigen retrieval	Positive control	Source
Calcitonin	Rabbit poly	1 in 600	Microwaving	Thyroid C-cell	Dako Denmark A/S, Glostrup, Denmark
CD31	Mouse mono (JC70)	Prediluted	Proteinase K[b)]	Endothelial cell of arteriole	Monosan, Uden, Netherlands
α-SMA	Mouse mono (1A4)	1 in 100	Microwaving	Smooth muscle cell of arteriole	Dako Denmark A/S, Glostrup, Denmark
Laminin	Rabbit poly	1 in 100	Protease[a)]	Basement membrane of arteriole	Thermo Fisher Scientific, Fremont, CA, U.S.A.
Fibronectin	Rabbit poly	1 in 400	Protease[a)]	Basement membrane of arteriole	Dako Denmark A/S, Glostrup, Denmark
Collagen type IV	Rabbit poly	1 in 100	Protease[a)]	Basement membrane of arteriole	Abcam, Cambridge, U.K.
Ki-67	Mouse mono (MIB-1)	1 in 50	Autoclaving	Esophagus	Dako Denmark A/S, Glostrup, Denmark
GLUT-1	Rabbit poly	1 in 200	Microwaving	Bladder	Abcam, Cambridge, U.K.
MCT-1	Chicken poly	1 in 200	Microwaving	Large intestine	Millipore, Billerica, MA, U.S.A.

a) Nichirei, Tokyo, Japan. b) Dako Denmark A/S, Glostrup, Denmark.

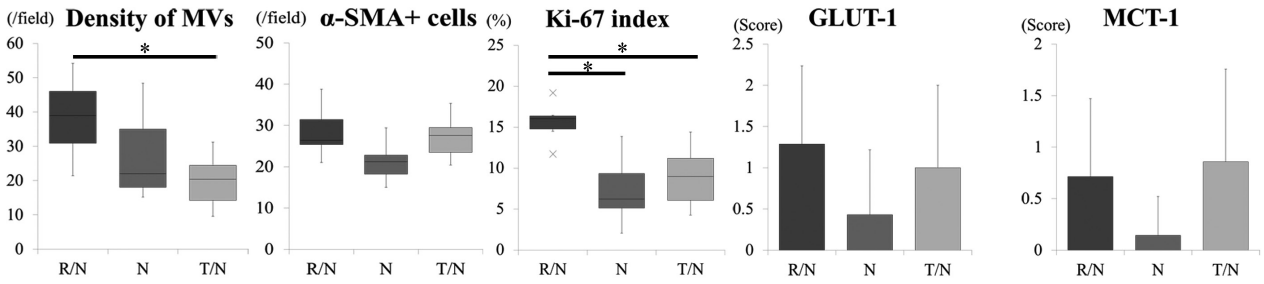

Fig. 9. Relationship of stroma variations with density of MVs, α-SMA-positive cell count, Ki-67 index, GLUT-1 and MCT-1. Box plots for the density of MVs, α-SMA-positive cell count and Ki-67 index in 3 stroma variations showing the interquartile range (25–75%). The line within the box is the median value. The bottom and top bars of the whisker indicate the minimum and maximum values. Outlier values are plotted as cross marks. The mean ± SD values of the GLUT-1 and MCT-1 expression scores of 3 stroma variations are shown (*P<0.05).

Macrovascular invasions were observed in 5 cases (R/N, 2; N, 2; and T/N, 1); on the other hand, microvascular invasions were observed in all 21 cases. Tumor cells with heteromorphic nuclei (nuclear pseudoinclusion body) were observed in 8 cases (R/N, 1; N, 3; and T/N, 4). Although mitotic figures were infrequent, 8 cases (R/N, 4; N, 3; and T/N: 1) were allocated to a high mitotic figure group (5–10/10HPF), and 13 cases (R/N, 3; N, 4; and T/N, 6) were allocated to a low mitotic group (1–4/10HPF).

MVs and stroma cells: Anti-CD31 antibody was used to clearly identify the endothelial cells of MVs in our study. In R types, CD31-positive endothelial cells of MVs were scattered among the tumor cells, and α-smooth muscle actin (SMA)-positive scattered stromal cells had dendritic cytoplasm (Fig. 4a and 4b). In N types, CD31-positive endothelial cells of MVs surrounded the tumor cells groups entirely, and α-SMA-positive spindle-shaped cells surrounded the entire circumference of tumor cell groups and adhered to basolateral surfaces (Fig. 5a and 5b). In T types, CD31-positive endothelial cells of MVs were poorly branched and penetrated through the thick collagenous bundles, and α-SMA-positive spindle-shaped linear cells were parallel, extending long and straight along the collagenous bundles (Fig. 6a and 6b). PAMS-positive reticular and collagenous fibers observed by histological examination and the cytoplasm of α-SMA-positive stroma cells were positive for anti-fibronectin, laminin and collagen type IV antibodies (Supplementary Figs. 1–3).

Density of MVs: Statistical analysis revealed significant differences among the 3 variations (P=0.027). The density of MVs in R/N was significantly higher than that in T/N (P=0.028), and no significant differences were found between R/N and N or between N and T/N (Fig. 9). Summaries of the mean ± standard deviation (SD) values in the semiquantitative analysis are shown in Supplementary Table 2.

α-SMA-positive cell count: Although a nonparametric test showed significant difference among the 3 variations (P=0.037), there was no significant difference by multiple comparison tests. The α-SMA-positive cell count in N tended to be less than those in R/N and T/N (Fig. 9). Summaries of the mean ± SD values in the semiquantitative analysis are shown in Supplementary Table 2.

Ki-67 index: Statistical analysis revealed significant differences among the 3 variations (P=0.003). Tumor cells in R/N had a significantly higher Ki-67 index compared with the tumor cells in N and T/N (vs. N, P=0.007; vs. T/N, P=0.03). There was no significant difference between N and T/N (P=0.89) (Fig. 9). Summaries of the mean ± SD values in the semiquantitative analysis are shown in Supplementary Table 2.

Expressions of GLUT-1 and MCT-1: Immunoreactions of GLUT-1 (Fig. 7) and MCT-1 (Fig. 8) were localized on the cytoplasmic membrane of tumor cells. The staining grade of GLUT-1 in the 3 variations ranged from 0 to 2, and the staining grade of MCT-1 in the 3 variations ranged from 0 to 2. Regarding the GLUT-1 and MCT-1 grades, statistical analysis of staining grades showed no significant difference among the 3 variations (P=0.23 and P=0.16), but the expression grades of N tended to decrease (Fig. 9). Summaries of immunoreactive scoring of GLUT-1 and MCT-1 are shown in Supplementary Table 2.

DISCUSSION

Our study is the first demonstration of detailed stroma components and their variations in CTCCs. Previous studies of thyroid C-cell (medullary) carcinomas uncovered various histological patterns, but the relation with cytological, histological and biological activity has remained unclear in humans and dogs [3, 13]. Growth patterns, appearance of heteromorphic nuclei and degree of mitotic figures on tumor parenchyma cells in CTCCs were not associated with stroma variations. Generally, a tumor's histological variation is determined based on differentiation or pleomorphic shapes of tumor parenchyma cells; however, it is difficult to differentiate thyroid C-cells. Therefore, our investigation provided a new viewpoint for distinguishing CTCCs histological variation.

The R type was defined by its high-density MVs with sheeted tumor cells. Although the fineness of the MVs made them difficult to recognize, PAMS was a useful tool for revealing them in a histological examination. The distribution, morphological features and number of α-SMA-positive cells having dendritic cytoplasm were correlated with MVs. These findings suggested that these α-SMA-positive cells, which were considered pericytes of MVs [11], might play a role in angiogenesis in the stroma of R type. The N type, which was most frequently observed in this study, exhibited a similarity with the "typical type" in a previous CTCCs study [13]. We suspected that the difference between the R and N types might or might not have resulted from infiltrating MVs among tumor cells. The α-SMA-positive cells in the stroma of the N type stroma had mature cytoplasm compared with the R type. Moreover, the number of MVs and α-SMA-positive cells tended to be fewer than in the R type. These findings suggested that the maturation of α-SMA-positive cells might be important in the regulation of MVs formation. The T types had mature fibrous connective tissue with a trabecular pattern of tumor cells and were mixed with nest types in many cases. Considering the increase of α-SMA-positive cells, which were considered myofibroblasts [10], without an increase of MVs compared with the N type, these findings suggested that a desmoplastic reaction without aggressive angiogenesis might have caused transformation from N to T type. In all types, α-SMA-positive cells and fibers defining the stroma types were expressing fibronectin, laminin and collagen type IV, which are known as major components of ECMs. This finding suggested that ECMs produced by α-SMA-positive cells might determine the composition of stroma types in CTCCs.

The correlation of stroma variations and the Ki-67 index in CTCCs was revealed in the present study. Although mitotic figures are generally thought of as an indicator of tumor cell proliferation, there is no usefulness for CTCCs because of the difficulty in identifying them. Ki-67 is a nuclear protein expressed in all cell cycle phases, except the resting phase. Therefore, we considered that almost all proliferating cells in CTCCs might be in interphase, not the M phase. This indicated that histological classification based on stroma variation might be useful for predicting tumor cell proliferation in CTCCs. The most interesting point in our study was that tumor cells having an R-type stroma demonstrated significantly higher cell proliferation compared with those having the other types. Moreover, although there was no significant difference, the Ki-67 index for the N/T variations tended to be higher than that for simple N variations. This tendency was similar to that found for the α-SMA-positive cell count. Therefore, we suggest that the morphological features and the number of α-SMA-positive stroma cells might be related to tumor cell proliferation in CTCCs. Although only a few studies in veterinary medicine have reported about α-SMA-positive stroma cells within carcinomas [4, 18], it is important and of interest to know how α-SMA-positive stroma cells affect stroma type and how they are regulated in tumors.

Our study demonstrated that the expressions of GLUT-1 and MCT-1 in R/N and T/N variations tended to be higher than that in simple N variations. This finding suggested that the classifications of stroma variations might reflect the expressions of these proteins. GLUT-1 and MCT-1 help tumor cells resist low glucose and acidic conditions [14, 15]. High expressions of these proteins in various canine malignant tumors, such as malignant melanomas, mammary gland carcinomas and histiocytic sarcomas, have been reported [1, 5, 15]; however, the current study is the first demonstration in CTCCs. Hypoxia-induced factor 1 (HIF-1) is an oxygen-sensitive protein that upregulates the expression not only of GLUT-1 and MCT-1 but also vascular endothelial growth factors (VEGFs), which promote angiogenesis [9, 14]. A previous study indicated that high VEGF expression is observed in all investigated cases of CTCC [2]. At first, we presumed high expressions of GLUT-1 and MCT-1 would also be observed in all cases; however, the expressions were different in each case and in each region of the same case. This suggested that there GLUT-1 and MCT-1 might have different mechanisms of expression compared with VEGF in CTCCs. A further study is needed to clarify this.

In conclusion, our study revealed that 3 stroma types are observed in CTCCs and that there are 3 stroma variations based on their combinations. R/N variations having abundant MVs indicate the highest tumor cell proliferation and high expressions of GLUT-1 and MCT-1; simple N variations, which are the most typical stroma type, indicate low tumor proliferation and expressions of GLUT-1 and MCT-1; and T/N variations having thick fibrous bundles with poor

MVs indicate low tumor proliferation and high expressions of GLUT-1 and MCT-1. Considering that the stroma types were mixed in many cases, it is important to investigate the histological stroma diversity in CTCCs to understand tumor cell activity.

ACKNOWLEDGMENTS. We would like to thank Patho LABO and the Veterinary Medical Center and Veterinary Teaching Hospital of Rakuno Gakuen University for their generous collaboration in sample collection.

REFERENCES

1. Abbondati, E., Del-Pozo, J., Hoather, T. M., Constantino-Casas, F. and Dobson, J. M. 2013. An immunohistochemical study of the expression of the hypoxia markers Glut-1 and Ca-IX in canine sarcomas. *Vet. Pathol.* **50**: 1063–1069. [Medline] [CrossRef]
2. Campos, M., Ducatelle, R., Kooistra, H. S., Rutteman, G., Duchateau, L., Polis, I. and Daminet, S. 2014. Immunohistochemical expression of potential therapeutic targets in canine thyroid carcinoma. *J. Vet. Intern. Med.* **28**: 564–570. [Medline] [CrossRef]
3. Desai, S. S., Sarkar, S. and Borges, A. M. 2005. A study of histopathological features of medullary carcinoma of the thyroid: cases from a single institute in India. *Indian J. Cancer* **42**: 25–29. [Medline] [CrossRef]
4. Destexhe, E., Lespagnard, L., Degeyter, M., Heymann, R. and Coignoul, F. 1993. Immunohistochemical identification of myoepithelial, epithelial, and connective tissue cells in canine mammary tumors. *Vet. Pathol.* **30**: 146–154. [Medline] [CrossRef]
5. Freeman, A., Hetzel, U., Cripps, P. and Mobasheri, A. 2010. Expression of the plasma membrane markers aquaporin 1 (AQP1), glucose transporter 1 (GLUT1) and Na, K-ATPase in canine mammary glands and mammary tumours. *Vet. J.* **185**: 90–93. [Medline] [CrossRef]
6. Halestrap, A. P. and Wilson, M. C. 2012. The monocarboxylate transporter family—role and regulation. *IUBMB Life* **64**: 109–119. [Medline] [CrossRef]
7. Harmelin, A., Nyska, A., Aroch, I., Yakobson, B., Stern, S., Orgad, U. and Waner, T. 1993. Canine medullary thyroid carcinoma with unusual distant metastases. *J. Vet. Diagn. Invest.* **5**: 284–288. [Medline] [CrossRef]
8. Lee, J. J., Larsson, C., Lui, W. O., Höög, A. and Von Euler, H. 2006. A dog pedigree with familial medullary thyroid cancer. *Int. J. Oncol.* **29**: 1173–1182. [Medline]
9. Majmundar, A. J., Wong, W. J. and Simon, M. C. 2010. Hypoxia-inducible factors and the response to hypoxic stress. *Mol. Cell* **40**: 294–309. [Medline] [CrossRef]
10. Mbeunkui, F. and Johann, D. J. Jr. 2009. Cancer and the tumor microenvironment: a review of an essential relationship. *Cancer Chemother. Pharmacol.* **63**: 571–582. [Medline] [CrossRef]
11. Morikawa, S., Baluk, P., Kaidoh, T., Haskell, A., Jain, R. K. and McDonald, D. M. 2002. Abnormalities in pericytes on blood vessels and endothelial sprouts in tumors. *Am. J. Pathol.* **160**: 985–1000. [Medline] [CrossRef]
12. Patnaik, A. K., Lieberman, P. H., Erlandson, R. A., Acevedo, W. M. and Liu, S. K. 1978. Canine medullary carcinoma of the thyroid. *Vet. Pathol.* **15**: 590–599. [Medline] [CrossRef]
13. Patnaik, A. K. and Lieberman, P. H. 1991. Gross, histologic, cytochemical, and immunocytochemical study of medullary thyroid carcinoma in sixteen dogs. *Vet. Pathol.* **28**: 223–233. [Medline] [CrossRef]
14. Romero-Garcia, S., Lopez-Gonzalez, J. S., Báez-Viveros, J. L., Aguilar-Cazares, D. and Prado-Garcia, H. 2011. Tumor cell metabolism: an integral view. *Cancer Biol. Ther.* **12**: 939–948. [Medline] [CrossRef]
15. Shimoyama, Y., Akihara, Y., Kirat, D., Iwano, H., Hirayama, K., Kagawa, Y., Ohmachi, T., Matsuda, K., Okamoto, M., Kadosawa, T., Yokota, H. and Taniyama, H. 2007. Expression of monocarboxylate transporter 1 in oral and ocular canine melanocytic tumors. *Vet. Pathol.* **44**: 449–457. [Medline] [CrossRef]
16. Watnick, R. S. 2012. The role of the tumor microenvironment in regulating angiogenesis. *Cold Spring Harb. Perspect. Med.* **2**: a006676. [Medline] [CrossRef]
17. Weidner, N., Semple, J. P., Welch, W. R. and Folkman, J. 1991. Tumor angiogenesis and metastasis—correlation in invasive breast carcinoma. *N. Engl. J. Med.* **324**: 1–8. [Medline] [CrossRef]
18. Yoshimura, H., Michishita, M., Ohkusu-Tsukada, K. and Takahashi, K. 2011. Increased presence of stromal myofibroblasts and tenascin-C with malignant progression in canine mammary tumors. *Vet. Pathol.* **48**: 313–321. [Medline] [CrossRef]